

# High $T_c$ superconductivity in superlattices of insulating oxides

D. Di Castro,<sup>1</sup> M. Salvato,<sup>2</sup> A. Tebano,<sup>1</sup> D. Innocenti,<sup>1</sup> C. Aruta,<sup>3</sup> W. Prellier,<sup>4</sup> O. I. Lebedev,<sup>4</sup> I. Ottaviani,<sup>2</sup> N. B. Brookes,<sup>5</sup> M. Minola,<sup>6</sup> M. Moretti Sala,<sup>6,5</sup> C. Mazzoli,<sup>6</sup> P.G. Medaglia,<sup>7</sup> G. Ghiringhelli,<sup>6</sup> L. Braicovich,<sup>6</sup> M. Cirillo,<sup>2</sup> and G. Balestrino<sup>1</sup>

<sup>1</sup>*CNR-SPIN and Dipartimento di Ingegneria Informatica Sistemi e Produzione,  
Università di Roma Tor Vergata, Via del Politecnico 1, I-00133 Roma, Italy*

<sup>2</sup>*Dipartimento di Fisica and MINAS Lab.,  
Università di Roma Tor Vergata, I-00133 Roma, Italy*

<sup>3</sup>*CNR-SPIN, Dipartimento di Scienze Fisiche,  
Via Cintia, Monte S. Angelo, 80126 Napoli, Italy*

<sup>4</sup>*Laboratoire CRISMAT, UMR 6508,  
CNRS-ENSICAEN 6Bd Marechal Juin, 14050 Caen, France*

<sup>5</sup>*European Synchrotron Radiation Facility, 6 rue Jules Horowitz,  
BP 220, 38043 Grenoble, Cedex 9, France*

<sup>6</sup>*CNISM and Dipartimento di Fisica,  
Politecnico di Milano, I-20133, Italy*

<sup>7</sup>*CNR-SPIN and Dipartimento di Ingegneria Industriale,  
Università di Roma Tor Vergata, Via del Politecnico 1, I-00133 Roma, Italy*

(Dated: March 16, 2012)

## Abstract

We report the occurrence of superconductivity, with maximum  $T_c = 40$  K, in superlattices (SLs) based on two insulating oxides, namely  $\text{CaCuO}_2$  and  $\text{SrTiO}_3$ . In these  $(\text{CaCuO}_2)_n/(\text{SrTiO}_3)_m$  SLs, the  $\text{CuO}_2$  planes belong only to  $\text{CaCuO}_2$  block, which is an antiferromagnetic insulator. Superconductivity, confined within few unit cells at the  $\text{CaCuO}_2/\text{SrTiO}_3$  interface, shows up only when the SLs are grown in a highly oxidizing atmosphere, because of extra oxygen ions entering at the interfaces. Evidence is reported that the hole doping of the  $\text{CuO}_2$  planes is obtained by charge transfer from the interface layers, which act as charge reservoir.

PACS numbers:

The parent compounds of high transition temperature ( $T_c$ ) cuprate superconductors (HTS) are antiferromagnetic insulators and develop superconductivity when charge carriers are introduced in the CuO<sub>2</sub> planes; this injection is usually achieved by charge transfer from a properly doped structural subunit (charge reservoir). A different approach to obtain high  $T_c$  superconductivity is based on the engineering of heterostructures (HSs) or superlattices (SLs) by advanced layer by layer deposition techniques. Up to now this approach has been applied to artificial structures consisting of an insulating and a metallic cuprate, such as CaCuO<sub>2</sub>/BaCuO<sub>2</sub> [1–3] and La<sub>2</sub>CuO<sub>4</sub>/La<sub>2-x</sub>Sr<sub>x</sub>CuO<sub>4</sub> [4, 5]. In these systems the metallic cuprate acts as charge reservoir, injecting carriers in the CuO<sub>2</sub> planes of the insulating cuprate, thus artificially reproducing the mechanism which naturally occurs in cuprate HTS.

Bearing in mind this mechanism one could speculate about different possible choices of the charge reservoir block, not necessarily a metallic cuprate. On the other hand, it has been shown that, by an adequate choice of the two constituent oxides, it is possible to realize a metallic interface, which can be itself superconducting, as in the case of the LaAlO<sub>3</sub>/SrTiO<sub>3</sub> HS [6]. This extraordinary interface phenomenon suggests that it could be possible to individuate the two systems, one copper oxide and one copper-free oxide, in order to obtain a doped interface, which could act as charge reservoir for the cuprate block. Following this idea we have chosen two insulating oxides, namely the SrTiO<sub>3</sub> (STO) and the CaCuO<sub>2</sub> (CCO), as building blocks for the engineering of (CCO)<sub>*n*</sub>/(STO)<sub>*m*</sub> SLs, where *n* and *m* are the number of unit cells (u.c.) of CCO and STO, respectively. SrTiO<sub>3</sub> is at the basis of the emerging field of oxide electronics because of the occurrence of exotic, two-dimensional phases of electron matter at the interface with other oxides [7–9]. CaCuO<sub>2</sub> is an antiferromagnetic insulator [10–12] and it is considered the simplest parent compound of HTS: in this compound the CuO<sub>2</sub> planes, where superconductivity can occur, are separated by bare Ca atoms in a pure infinite layer (IL) structure [10]. In this Letter, we provide evidences that, when these two model systems are brought together to form the superlattice (CCO)<sub>*n*</sub>/(STO)<sub>*m*</sub>, superconductivity, with a maximum  $T_c = 40$  K (zero resistance temperature), is achieved. The interfaces, hybrid between perovskite and infinite layer structure, can leave space for extra oxygen ions to come in and dope the system. The charge reservoir is thus likely provided by the interface layers, which inject holes in the inner CuO<sub>2</sub> planes of the CCO block, making the SLs superconducting, although constituted by two insulating materials.

We used pulsed laser deposition to synthesize several superlattices (CCO)<sub>*n*</sub>/(STO)<sub>*m*</sub>,

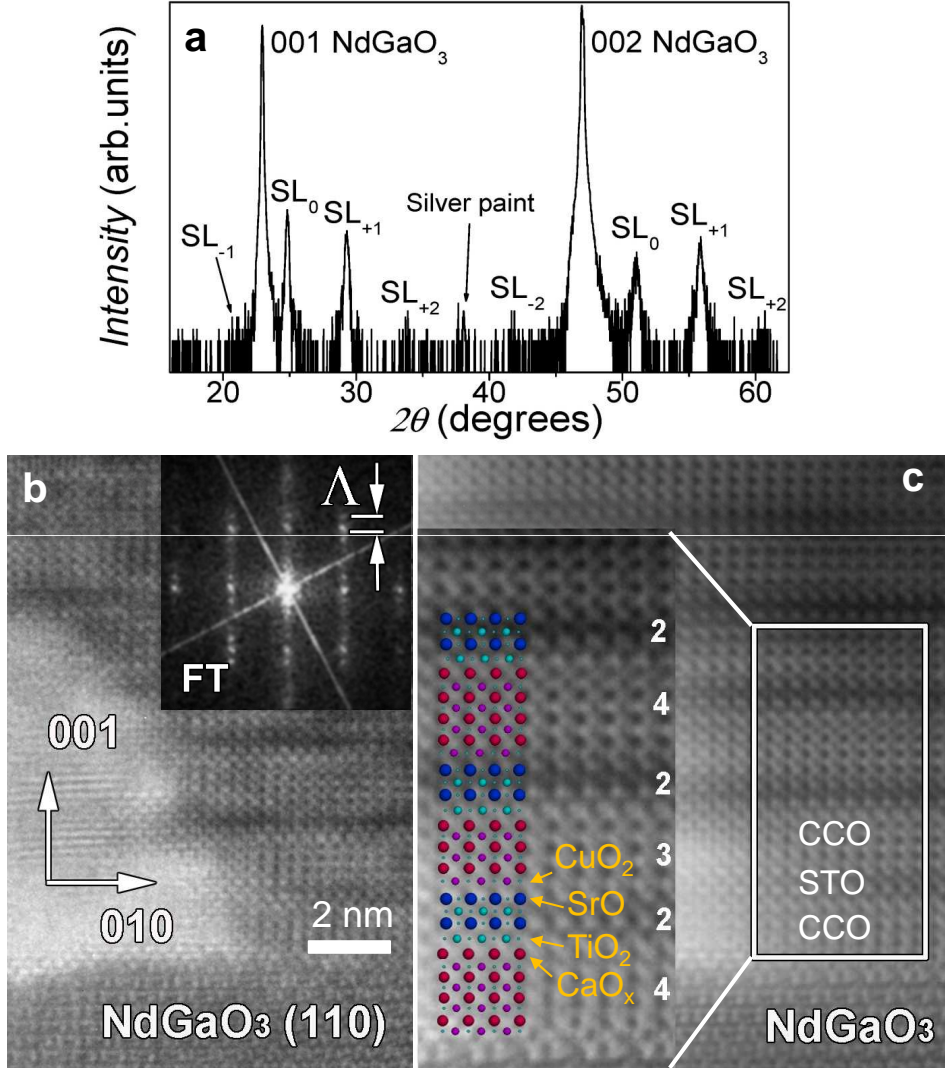


FIG. 1: a) XRD pattern (intensity in log scale) from  $(\text{CaCuO}_2)_{3.5}/(\text{SrTiO}_3)_2$  SL.  $\text{SL}_{\pm i}$  mark the satellite peaks, around the average structure peak  $\text{SL}_0$ . b) HRTEM image of identical SL taken along the [110] orientation of the NdGaO<sub>3</sub> substrate. Inset: Fourier Transform pattern where superlattice spots are clearly visible along [001] growth direction. c) filtered HRTEM image. Inset: enlargement of the area marked by white rectangle close to substrate with the atomic model of STO-CCO sequences (dark blue: Sr; light blue: Ti; small light blue: O; red: Ca; purple: Cu).

made by 10 to 20 repetitions of  $n$  unit cell of CCO and  $m$  unit cells of STO, on NdGaO<sub>3</sub>(110) (NGO) substrate. NGO is the most suitable substrate to grow both CCO [13] and STO, having a pseudocubic in plane lattice parameter ( $a = 3.87 \text{ \AA}$ ) just in the middle between CCO

( $a = 3.84 \text{ \AA}$ ) and STO ( $a = 3.91 \text{ \AA}$ ). The superconducting SLs were grown at about  $600^\circ\text{C}$  in a mixture of oxygen and 12% ozone atmosphere at a pressure of about 1 mbar. The growth was followed by a quenching at an oxygen pressure of about 1 bar (details in Supplemental Materials [14]). In Fig.1a the x-ray diffraction (XRD) spectrum of a superconducting SL  $(\text{CCO})_n/(\text{STO})_m$ , with nominal composition  $n = 3$  and  $m = 2$ , reveals the presence of sharp satellite peaks around the average structure one, indicating the formation of a high quality superlattice with period  $\Lambda \approx 19.5(5) \text{ \AA}$ ,  $n = 3.5(5)$ , and  $m = 2.0(5)$  (see also Fig.S1 in Supplemental Materials [14]). To better evaluate the structural quality of CCO/STO SLs, we recorded a HRTEM image (details in Supplemental Material [14]) on an identical sample along the [110] direction of the  $\text{NdGaO}_3$  substrate. The image (Fig.1b) shows a heteroepitaxial superlattice film growth and a series of stacked layers with different contrast, regularly alternate thicknesses and sharp interfaces. The high quality of the SL is confirmed by the Fourier Transform (FT) pattern (inset of Fig.1b), where, beside the intense reflections associated with the CCO and STO substructures, satellite lower intensity reflections are observed in the growth direction (i.e. [001]\* direction). These reflections are associated to the periodic structure generated by the regular stacking of CCO and STO. The stacking can be described as an average of 3.5 u.c. of CCO and 2 u.c. of STO, with a superlattice period  $\Lambda \approx 19 \text{ \AA}$ , in agreement with the XRD analysis. This means that the number of CCO u.c. varies from 3 to 4. This assignment is confirmed by the analysis of the filtered HRTEM image (see Fig.1c), where it is possible to precisely determine the layers stacking, as illustrated in the color circles model structure in the inset.

We have observed that the conductivity of  $(\text{CCO})_n/(\text{STO})_m$  SLs slightly varies with varying  $n$  and  $m$ , but increases substantially with increasing the oxidizing power of the growth atmosphere, till the occurrence of superconductivity. In particular, we have found that for a weakly oxidizing growth atmosphere (oxygen pressure lower than 0.1 mbar) the SLs show always a semiconductor-like temperature dependence of the resistance (Fig. 2c), even if the film is quenched to room temperature in high (about 1 bar) oxygen pressure. An insulator to metal transition occurs only when a highly oxidizing growth atmosphere is used (oxygen plus 12% ozone at a pressure of about 1 mbar) and the film is rapidly quenched to room temperature at high oxygen pressure (about 1 bar). Under these conditions, the SL is metallic, and, in the best case, the resistance goes to zero at about 40 K (Fig. 2c). Thus, strong oxidation is a key ingredient to obtain superconducting samples.

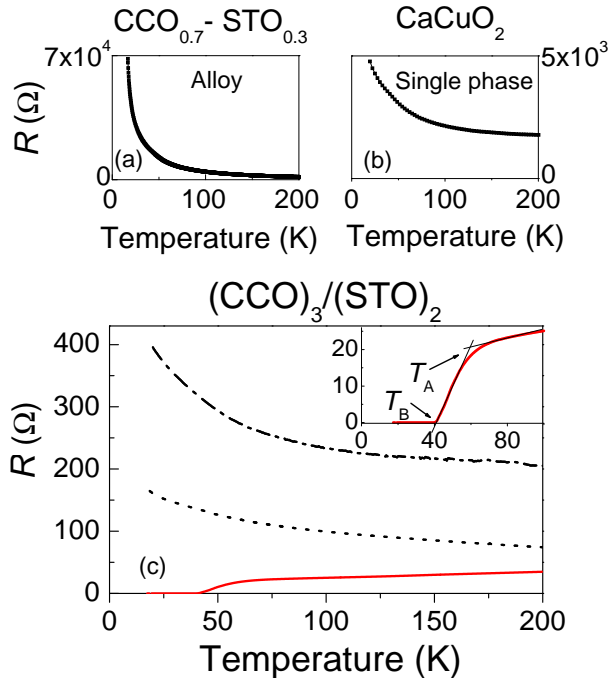


FIG. 2: (color online) Temperature dependencies of the resistance of the alloy CCO-STO (a) and single phase CCO (b) grown in the same conditions as the superconducting SLs. c)  $R(T)$  for a SL grown in low oxidizing atmosphere (dash-dotted line), for one grown in the same condition and quenched in high (about 1 bar) oxygen pressure (dotted line), and for a SL grown in a oxygen/ozone mixed atmosphere at higher pressure and quenched in high oxygen pressure (full line). Inset: superconducting transition shown on a reduced temperature range. The width of the transition, defined as  $T_A - T_B$ , for all the SLs ranges between 4 K and 18 K.

The occurrence of superconductivity has been also probed by magnetization measurements, performed using a commercial SQUID by Quantum Design. Since the NGO substrate is strongly paramagnetic [15], and, at low temperature, it hinders the detection of the diamagnetic signal from the SL, then, as a substrate, we used LaAlO<sub>3</sub> (LAO), which has a small and temperature independent diamagnetism [16] (see Fig.3a). A clear signature of diamagnetic transition in (CCO)<sub>3</sub>/(STO)<sub>2</sub> SL does appear below 12 K. The  $T_c$  in this SL is much depressed compared to similar SLs grown on NGO, probably because of the larger and opposite in-plane lattice mismatch between LAO ( $a = 3.78 \text{ \AA}$ ) and CCO.

In order to check the robustness of the superconducting phenomenon, critical current

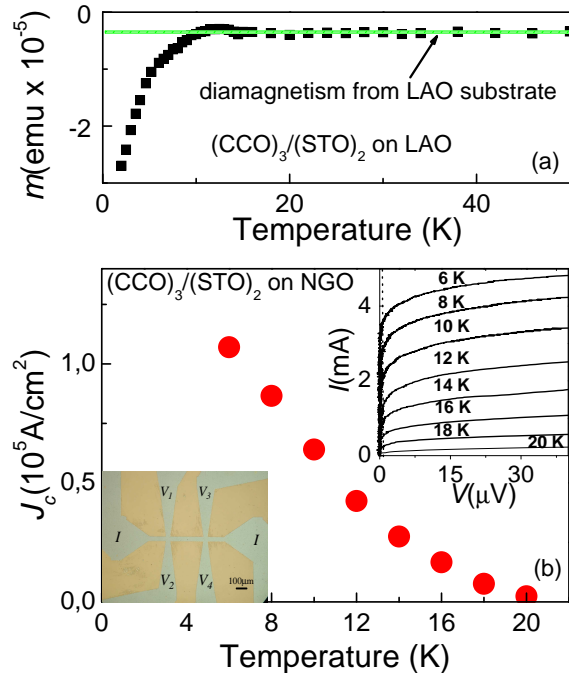


FIG. 3: (color online) a)Magnetic moment as a function of temperature for a  $(\text{CCO})_3 /(\text{STO})_2$  SL grown on  $\text{LaAlO}_3$  substrate. The horizontal line indicates the temperature independent diamagnetism of the LAO substrate. b) Critical current density as a function of temperature for a sample  $(\text{CCO})_3 /(\text{STO})_2$  with  $T_c = 22 \text{ K}$  after patterning process. Right up inset:  $V - I$  characteristics at different temperature for the sample shown in left bottom inset. The vertical dashed line is drawn at  $V=1\mu\text{V}$ , which corresponds to the criterion adopted for  $I_c$  measurement. Left bottom inset: patterned sample for  $V - I$ , resistivity, and Hall effect measurements.

density ( $J_c$ ) measurements were performed on patterned samples (details in Supplemental Material [14]). A picture of a patterned sample ( $T_c = 22 \text{ K}$  after the patterning process) is reported in the lower inset of Fig.3b. The  $I$ - $V$  characteristics are shown in the upper inset of Fig.3b at different temperatures, from which we obtained the temperature dependence of  $J_c$  shown in the main panel. At  $T = 6 \text{ K}$ ,  $J_c = 1.1 \times 10^5 \text{ A}/\text{cm}^2$ . The same kind of measurements on similar samples give  $J_c$  values of the same order, independently on the length and the width of the strip. Comparable  $J_c$  values have been found in other superconducting SLs consisting of a metallic and a superconducting cuprates [4]. The measured resistivity at  $T = 300 \text{ K}$  is  $1.5 \text{ mOhm}\cdot\text{cm}$ , a value typical for HTS [17].

Now, it is important to point up that the proper doping and the consequent superconductivity do occur only in the presence of a layered structure with sharp interfaces. Indeed, we have grown, in the same strongly oxidizing conditions used for the superconducting SLs, a CCO-STO alloy (interface free), with 70% CCO and 30% STO, and a pure CCO film: both systems show a semiconductor-like temperature dependence of the resistance with no trace of superconductivity (see Fig. 2a and 2b). Therefore, the *layered structure* is needed in order to obtain superconductivity, and we can thus argue that the excess oxygen atoms enter at the CCO/STO interfaces.

In CCO/STO SLs two interfaces can be envisaged (see bottom inset of Fig.1b): Ca-CuO<sub>2</sub>-SrO-TiO<sub>2</sub> and CuO<sub>2</sub>-Ca-TiO<sub>2</sub>-SrO. Apical oxygens for Cu are thus naturally present at the interface Ca-CuO<sub>2</sub>-SrO-TiO<sub>2</sub>, due to the oxygen atoms in the SrO plane. Both the interfaces are hybrid between the perovskite and the IL structure. In particular, the CuO<sub>2</sub>-Ca-TiO<sub>2</sub>-SrO interface could adopt the perovskite structure of CaTiO<sub>3</sub> or the IL structure of CaCuO<sub>2</sub>, both stable compounds in form of thin film. Therefore, it is likely that, under strongly oxidizing conditions, this interface becomes CuO<sub>2</sub>-CaO<sub>x</sub>-TiO<sub>2</sub>. Each of the excess oxygen atoms in the CaO<sub>x</sub> plane at the interface would contribute to doping.

Since we expect that the doping might occur at the interface, we investigate now how far from the interfaces superconductivity extends. To this aim we prepared a series of SLs, where the number of STO unit cells is kept fixed at  $m = 2$  and the number of CCO unit cells is varied from  $n \approx 1.5$  to  $n \approx 20$ . Superconductivity shows up when  $n$  becomes larger than 2, and  $T_{cm}$ , defined as the transition midpoint in the  $R(T)$  curves (inset to Fig.4a), reaches the maximum value of 50 K for  $n$  between 3 and 4 (Fig. 4a), that is for 3 CuO<sub>2</sub> planes. This is in agreement with the behavior of HTSs, which, within each cuprate family, show the highest  $T_c$  in the trilayer systems [23]. For higher values of  $n$ ,  $T_{cm}$  decreases and, for  $n > 5$  remains almost constant up to the thickest sample ( $n \approx 20$ ). This behavior suggests that superconductivity is confined within few unit cells from the interface. To further confirm this conclusion, we analyzed the sheet resistance  $R_s$  multiplied by the number of CCO layer  $N$ :  $R_s^l = N \times R_s$ , i.e., the sheet resistance per CCO layer (see also Supplemental Material [14]). If transport was uniform over the whole CCO layer it would result in a linear dependence of  $R_s^l$  on the inverse of the number  $n$  of CCO unit cells, extrapolating to  $R_s^l = 0$  at  $n^{-1} = 0$ . Actually, Fig. 4b shows that  $R_s^l$  does not change with increasing CCO thickness, but for the point referring to the SL with the thinnest CCO block, thus pointing towards a

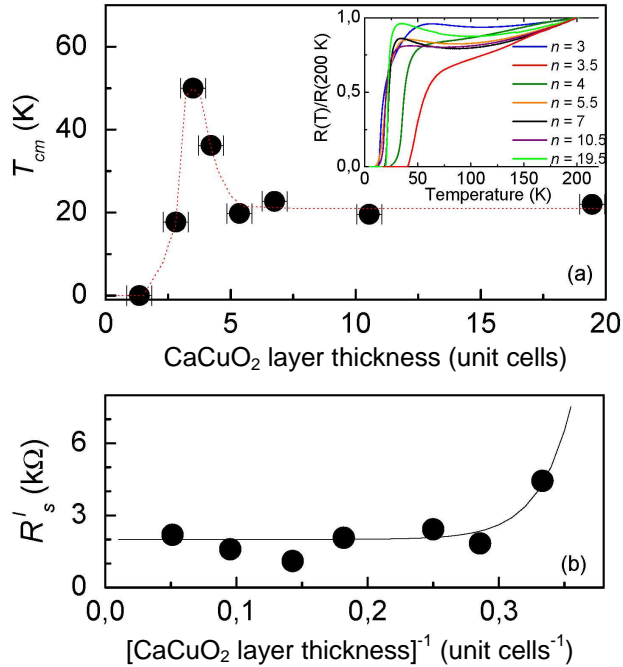


FIG. 4: (color online) a)  $T_{cm}$ , defined as the midpoint of the resistive transitions shown in the inset, as a function of the number of unit cells of the CCO layer for various SLs with different number  $n$  of CCO unit cells. The dotted line is a guide for the eye. Inset:  $R(T)$  normalized at  $T = 200$  K for the same SLs as in the main panel. b) sheet resistance at 80 K of a single CCO layer  $R_s^l$  as a function of the inverse of the number of CCO unit cells. Full line is a guide to the eye.

(super)conductivity close to the interface.

In the remainder of the paper we shall present the results of experiments, performed with the aim to determine the nature (holes or electrons) of the doping charge carriers and where these are located (which could be either on Cu- or Ti-bands).

In order to probe the nature of the carriers, Hall voltage ( $V_H$ ) measurements were performed on suitably patterned samples (see inset to Fig.3b).  $V_H$  was measured at room temperature between the opposite voltage contacts biasing the sample with a  $100 \mu\text{A}$  dc current and applying an external magnetic field  $B$  up to 1.2 T (more details on this measurement in Supplemental Material [14]). A positive Hall constant  $R_H = 3.4 \times 10^{-3} \text{ cm}^3/\text{C}$  was obtained by linear interpolation of the  $V_H$  vs.  $B$  experimental data at fixed bias current (see Fig.S3 in Supplemental Material). The positive sign of  $R_H$  gives a strong indication

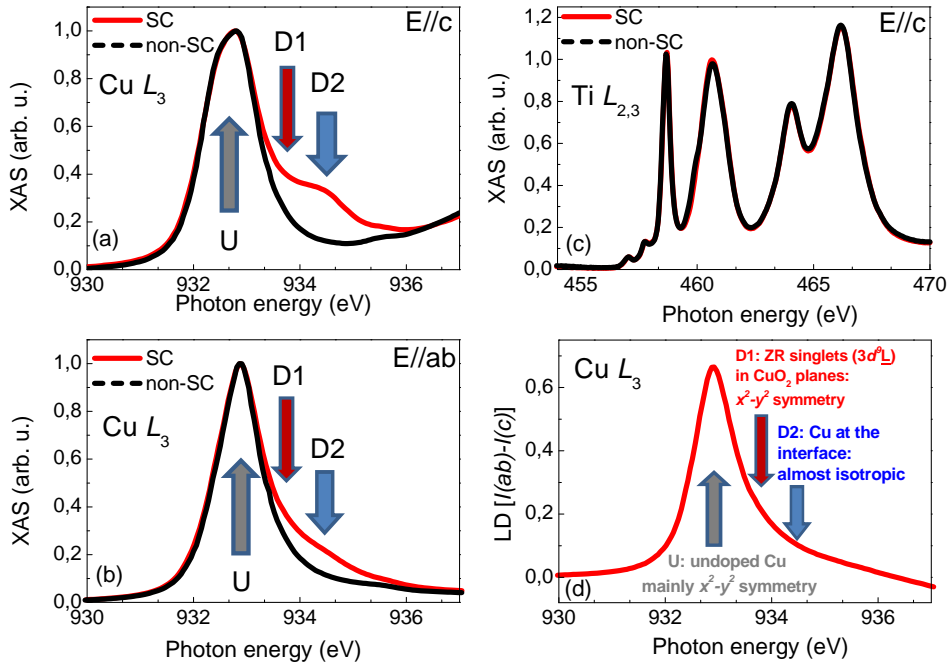


FIG. 5: (color online) a,b: Cu  $L_3$ -edge for a superconducting (SC) (full line) and non-superconducting (dashed line)  $(\text{CCO})_3/(\text{STO})_2$  SL. All measurements are performed at  $T = 5$  K in both the polarizations  $E//c$ -axis (panel a) and  $E//ab$ -plane (panel b) and the spectra are normalized to the maximum height intensity of the  $L_3$  edge. c) the two multiplets Ti  $L_2$ - and Ti  $L_3$  - edges for SC and non-SC sample. d)linear dichroism for the SC sample.

of the hole nature of the majority charge carriers in these materials. The calculated charge density is  $n_H = 1.8 \times 10^{21} \text{ cm}^{-3}$ , which results comparable with that observed in other cuprate superconductors and cuprate based SLs [17].

One of the original characteristic of the CCO/STO SLs, with respect to other previously reported high  $T_c$  HSs [1–5], is that in CCO/STO Cu is present only in one of the two constituent blocks. In this case a block selective study is possible by resonant spectroscopic techniques. Indeed, to individuate where the holes are located and to better understand the doping mechanism, we additionally performed x-ray absorption spectroscopy (XAS) measurements [3, 18] on the beamline ID08 at ESRF (for technical details see Supplemental Material [14]). XAS spectra were collected at the Cu and Ti  $L_{2,3}$ -edges on a superconducting  $(\text{CCO})_3/(\text{STO})_2$  SL with  $T_c$  ( $R=0$ ) = 25 K, and on an identical SL, but *non-superconducting*, since grown with no ozone and with no quenching at high oxygen pressure. Figs. 5a and

5b show the normalized XAS spectra taken at the Cu  $L_3$ -edge (Cu  $2p \rightarrow$  Cu  $3d$  electron transition energy) for the two samples with the electric field of the incident radiation parallel to the c-axis ( $\mathbf{E} \parallel c$ ) and to the ab-plane ( $\mathbf{E} \parallel ab$ ), respectively. The  $L_3$  peak at 932.5 eV, indicated with U in Fig.5, is associated to the process  $3d^9 \rightarrow \underline{c}3d^{10}$  ( $\underline{c}$  indicates a Cu  $2p$  core hole) and assigned to the absorption by an undoped Cu site [3, 19]. The tail D1 and the peak D2 about 1 eV and 1.5 eV above the main peak U, respectively, are associated to the process  $3d^9 \underline{L} \rightarrow \underline{c}3d^{10} \underline{L}$ , where  $\underline{L}$  indicates the oxygen ligand hole arising from Cu  $3d - O 2p$  hole, mainly with an O  $2p$  character [18]. Thus, these two features are assigned to the absorption by *hole* doped Cu sites [3, 19]. The major differences between the spectra of superconducting and non-superconducting SL are observed in the region around D1 and D2. In both polarizations, this region acquires spectral weight in the case of superconducting SL, as a clear indication of increased holes concentration delocalized on the in-plane and out-of-plane O  $2p$  bands [3, 19]. On the other hand, at the Ti  $L_{2,3}$  – edges, no relevant changes are observed between the superconducting and the non-superconducting samples (Fig.5c). According to ref. 20, in case of  $Ti^{3+}$  doping, an increase of the intensity would be expected in the region between the peak at 464 eV, associated to the  $3d-t_{2g}$  final states, and the peak at 466 eV, associated to the  $3d-e_g$  final state. This increase, in our case, does not occur. Therefore, not only the valence, but also the crystal-field in the Ti environment [20] are not substantially affected by the strongly oxidizing conditions used to obtain the superconducting sample.

With the help of the Cu- $L_3$ -edge linear dichroism (LD) showed in Fig. 5d, a more detailed assignment of the spectral features observed in Fig.5a and Fig.5b can be made in analogy to what was done for  $YBa_2Cu_3O_{7-\delta}$  (YBCO) in Refs. 21 and 22. The XAS LD (Fig.5d) is the difference between the XAS contributions from the two polarizations:  $LD = I(\mathbf{E} \parallel ab) - I(\mathbf{E} \parallel c)$ , where both the intensities have been normalized to the value of the  $L_3$  intensity of the  $\mathbf{E} \parallel ab$  spectrum. Thus, LD is a measure of the anisotropy of the environment around selected ions. In the SLs CCO/STO we do not expect to have chains, as in YBCO, but definitively we can distinguish two distinct Cu sites: i) interface sites Cu(1), which mostly are expected to have rather isotropic hole orientation due to the presence of the apical oxygen ion in the undoped SrO plane, at the Ca-Cu(1)O<sub>2</sub>-SrO-TiO<sub>2</sub> interface, and in the doped CaO<sub>x</sub> plane, at the Cu(1)O<sub>2</sub>-CaO<sub>x</sub>-TiO<sub>2</sub>-SrO interface. Less isotropic Cu(1) sites are expected at the Cu(1)O<sub>2</sub>-Ca-TiO<sub>2</sub>-SrO interfaces with no oxygen ions in the Ca plane;

ii) Cu(2) sites inside the CCO block ( $\text{Ca-Cu}(2)\text{O}_2\text{-Ca-Cu}(2)\text{O}_2\cdots$ ), with no apical oxygen ions at all, which are expected to have in plane (thus anisotropic) holes ( $x^2-y^2$  symmetry), both for doped and undoped sites. The main peak (U) at 932.8 eV is highly anisotropic (large LD), and it is assigned to the process  $3d^9 \rightarrow \underline{c}3d^{10}$  at undoped interface Cu(1) sites ( $\text{Cu}(1)\text{O}_2\text{-Ca-TiO}_2\text{-SrO}$  interface), and at undoped Cu(2) sites. On the contrary the feature at 934.5 eV (D2) is almost equally intense in the two polarizations (low LD) and we assign it to the  $3d^9\underline{\text{L}} \rightarrow \underline{c}3d^{10}\underline{\text{L}}$  process at the doped interface Cu(1) sites ( $\text{CuO}_2\text{-CaO}_x\text{-TiO}_2\text{-SrO}$  interface). The more anisotropic shoulder at 933.7 eV (D1) corresponds to  $3d^9\underline{\text{L}} \rightarrow \underline{c}3d^{10}\underline{\text{L}}$  process at doped Cu(2) sites, i.e., Zhang Rice singlets in the  $\text{CuO}_2$  planes. When oxygen is added at the interfaces, the doping holes, although mainly confined at Cu(1) sites, get transferred to the neighboring  $\text{Cu}(2)\text{O}_2$  planes, giving rise to superconductivity. After this LD analysis it is plausible to conclude that the role of charge reservoir, performed by Cu-O chains in YBCO, is played by the interface layers in CCO/STO superlattices.

In conclusion, we synthesized a novel superconducting material, with maximum  $T_c = 40$  K, by alternating an insulating IL cuprate,  $\text{CaCuO}_2$ , and a copper-free wide gap semiconductor,  $\text{SrTiO}_3$ , to form the superlattice  $(\text{CaCuO}_2)_n/(\text{SrTiO}_3)_m$ . Here, the charge reservoir role is played by the CCO/STO interfaces, due to the peculiar structural and electronic properties of the constituent oxides, which allow extra oxygen ions entering the interface planes. The doping charges resulted to be hole-type. These holes, from the interface layers, are injected in the inner  $\text{CuO}_2$  planes close to the interface, whereas STO does not contribute to transport. We believe that this work could motivate the search for other cuprate/non-cuprate synthetic heterostructures, in which the  $\text{CuO}_2$  plane properties (in-plane Cu-O distance, buckling), the charge reservoir characteristics, and the out-of plane unit cell size can be independently controlled. This possibility may lead to improved superconducting properties of the HSs and to unveil open questions concerning superconductivity in cuprates.

W.P. and O.I.L. are grateful to Dr. A. Pautrat for helpful discussion and to M. L. Gouleuf for the preparation of the samples for HRTEM measurements. D.D.C. thanks A. Maisuradze for support during magnetization measurement. C.A. and D.D.C. thanks J. Zeghenagen for fruitful discussions. This work was partly supported by the Italian MIUR (Grant No. PRIN-20094W2LAY, "Ordine orbitale e di spin nelle eterostrutture di cuprati e manganiti").

- 
- [1] G. Balestrino *et al.* *Phys. Rev. B* **58**, R8925 (1998);
  - [2] G. Balestrino *et al.* *Phys. Rev. B* **62**, 1421 (2000)
  - [3] C. Aruta *et al.* *Phys. Rev. B* **78**, 205120 (2008).
  - [4] A. Gozar *et al.* *Nature* **455**, 782-785 (2008).
  - [5] S. Smadici *et al.* *Phys. Rev. Lett.* **102**, 107004 (2009).
  - [6] N. Reyren *et al.* *Science* **317**, 1196-1199 (2007).
  - [7] C. Cen *et al.* *Science* **323**, 1026-1030 (2006).
  - [8] E. Dagotto, *Science* **318**, 1076-1077 (2006).
  - [9] A. P. Ramirez, *Science* **315**, 1377-1378 (2006).
  - [10] T. Siegrist *et al.* *Nature* **334**, 231 (1988).
  - [11] M. Takano *et al.* *Physica C* **176**, 441 (1991).
  - [12] S.J.L. Billinge *et al.* *Phys. Rev. B* **43**, 10340 (1991).
  - [13] G. Balestrino *et al.* *J. Mater. Chem.* **5**, 1879 (1995).
  - [14] See Supplemental Material at <http://link.aps.org/> supplemental for more details on the growth and on the structural and transport characterization of the SLs, on  $J_c$ , Hall effect and XAS measurements.
  - [15] A. Podlesnyak *et al.* *J. Phys.: Condens. Matter* **5**, 8973-8982 (1993).
  - [16] M. Khalid *et al.* *Phys. Rev. B* **81**, 214414 (2010).
  - [17] M. Affronte *et al.* *Phys. Rev. B* **43**, 11484 (1991)
  - [18] J. Fink *et al.* *Electron Spectrosc. Relat. Phenom.* **66**, 395 (1994).
  - [19] D. D. Sarma *et al.* *Phys. Rev. B* **37**, 9784 (1988)
  - [20] J. Verbeeck *et al.* *Phys. Rev. B* **81**, 085113 (2010)
  - [21] D. G. Hawthorn *et al.* *Phys. Rev. B* **84**, 075125 (2011).
  - [22] M. Merz *et al.* *Phys. Rev. Lett.* **80**, 5192 (1998).
  - [23] B. A. Scott *et al.* *Physica C* **230**, 239–245 (1994).